The TC10-interacting protein CIP4/2 is required for insulin-stimulated Glut4 translocation in 3T3L1 adipocytes

Louise Chang, Rachael D. Adams, and Alan R. Saltiel*

Departments of Internal Medicine and Physiology, Life Sciences Institute, University of Michigan Medical Center, Ann Arbor, MI 48109

Communicated by Pedro M. Cuatrecasas, University of California at San Diego School of Medicine, La Jolla, CA, August 16, 2002 (received for review July 20, 2002)

The GTPase TC10 plays a critical role in insulin-stimulated glucose transport. We report here the identification of the TC10-interacting protein CIP4/2 (Cdc42-interacting protein 4/2) as an effector in this pathway. CIP4/2 localizes to an intracellular compartment under basal conditions and translocates to the plasma membrane on insulin stimulation. Overexpression of constitutively active TC10 brings CIP4/2 to the plasma membrane, whereas overexpression of an inhibitory form of TC10 blocks the translocation of CIP4/2 produced by insulin. Overexpression of mutant forms of CIP4/2 containing an N-terminal deletion or with diminished TC10 binding inhibits insulin-stimulated Glut4 translocation. These data suggest that CIP4/2 may play an important role in insulin-stimulated glucose transport as a downstream effector of TC10.

Insulin stimulates glucose uptake in muscle and fat cells via the translocation of the facilitative transporter Glut4 from intracellular sites to the plasma membrane. The signaling events that regulate these processes are initiated by the receptor–catalyzed tyrosine phosphorylation of intracellular substrates. These include the insulin receptor substrate (IRS) proteins, which interact with phosphatidylinositol 3-kinase (PI3-kinase), leading to the activation of the enzyme (1, 2). The activation of PI3-kinase is required, but not sufficient for the stimulation of glucose transport (reviewed in ref. 3). The receptor also catalyzes the tyrosine phosphorylation of the protooncogene *c-cbl* (4). Cbl is recruited to the insulin receptor by the adapter protein APS [adapter containing pleckstrin homology domain and Src homology (SH) 2 domain; ref. 5] along with a second adapter protein CAP (Cbl-associated protein; refs. 6 and 7). The COOH-terminal SH3 domain of CAP associates with the proline-rich domain of Cbl, whereas its amino-terminal SH domain interacts with the lipid raft protein flotillin, stabilizing the complex in this plasma membrane subdomain (6, 7). Activation of both the IRS/PI3-kinase and APS/CAP/Cbl pathways are necessary for the stimulation of glucose transport and Glut4 translocation by insulin in 3T3L1 adipocytes (3, 8).

After its tyrosine phosphorylation in response to insulin, Cbl interacts with the SH2/SH3-containing adapter protein CrkII, subsequently producing the translocation of this molecule to lipid rafts, in the process also translocating the guanyl nucleotide exchange factor C3G. After translocation to the lipid raft subdomain, C3G activates the Rho family proteins TC10α and TC10β (9–11). Activation of TC10 by insulin requires the translocation of Cbl, CrkII, and C3G to lipid rafts, but is independent of the PI3-kinase pathway (12). Moreover, TC10 activation plays a crucial role in the stimulation of glucose transport by insulin (10, 12).

To further characterize the role of TC10 in insulin-stimulated glucose transport, we searched for potential effector molecules by using a yeast two-hybrid screen. We describe here one such protein, CIP4/2 (Cdc42-interacting protein 4/2). CIP4/2 is recruited to the plasma membrane in response to insulin and plays a crucial role in the regulation of insulin-stimulated Glut4 translocation.

Materials and Methods

Cell Culture. COS-1 cells were transfected with FuGene6 reagent following the manufacturer's instructions (Roche Diagnostics). 3T3L1 adipocytes were cultured as described (13, 14) and transfected by electroporation as described (15). For immunolocalization studies, adipocytes were electroporated with 100 μg plasmid expressing myc-CIP4/2 or its deletion mutants. For effects of TC10 overexpression on CIP4/2 cellular localization, adipocytes were electroporated with 200 μg TC10 or its mutants and 100 μg plasmid expressing myc-CIP4/2. For Glut4 translocation assays, adipocytes were coelectroporated with 50 μg plasmid expressing Glut4-enhanced GFP (eGFP) and 300 μg plasmid expressing FLAG-CIP4/2 or its deletion mutants. The electroporated cells were plated and allowed to recover for 30 h, serum-starved for 3 h, and treated with or without hormone at 37°C.

Yeast Two-Hybrid Screen. The cDNA of full-length human TC10 ($Q^{75}L$) was amplified by PCR using the plasmid pKH3-TC10($Q^{75}L$) (a gift from Ian Macara, University of Virginia, Charlottesville) as a template. The PCR product was then subcloned into an *Eco*RI/*Bam*HI site of the bait vector pGBT9 (CLONTECH), in-frame with the coding region of the GAL4 DNA binding domain. To screen for TC10-interacting proteins, yeast strain Y190 was sequentially transformed with bait DNA and then the yeast two-hybrid cDNA library derived from 3T3L1 adipocyte mRNA (16). The transformants were plated onto synthetic media lacking tryptophan, leucine, and histidine and containing 25 mM 3-aminotriazole (Sigma) and incubated at 30°C. Colonies were analyzed for β-galactosidase activity. Prey plasmids isolated from 5-bromo-4-chloro-3-indolyl β-D-galactoside (X-Gal)-positive colonies were retransformed into Y190 carrying the bait plasmid to confirm yeast two-hybrid interaction, and cDNA inserts were sequenced. All sequences were analyzed by the Basic Local Alignment Sequence Search Tool (BLAST) and the Simple Molecular Architecture Research Tool (SMART) (17–19).

Expression Constructs. To generate a mammalian expression vector, full-length CIP4/2 cDNA from the yeast two-hybrid clone was subcloned into *Eco*RI/*Xho*I sites of pCS2 in-frame with the myc N-terminal epitope tag-coding region. To generate deletion constructs, CIP4/2 was PCR-amplified from pGBT9 CIP4/2, and *Eco*RI/*Xho*I restriction sites were introduced into the primers, and then subcloned into pCS2 at *Eco*RI/*Xho*I. To generate GST fusion proteins, CIP4/2 full-length cDNA and its

Abbreviations: PI3-kinase, phosphatidylinositol 3-kinase; SH, Src homology; HA, hemagglutinin; CIP, Cdc42-interacting protein; FCH, FER-CIP4 homology; WASP, Wiskott–Aldrich syndrome protein; eGFP, enhanced GFP.

Data deposition: The sequence reported in this paper has been deposited in the GenBank database (accession no. AF502565).

*To whom reprint requests should be addressed. E-mail: saltiel@umich.edu.

deletion constructs were subcloned into *Eco*RI/*Xho*I sites of pGEX5X-1 in-frame with the GST N-terminal coding region. To generate CIP4/2 epitope tagged with FLAG at the N terminus, full-length CIP4/2 and the deletion constructs were PCR-amplified by using primers containing *Eco*RI sites. The PCR products were then subcloned into pFLAG-CMV2 (a gift from Greg Dressler, University of Michigan, Ann Arbor) in-frame with the FLAG coding region. To generate pCS2 CIP4/2ΔGBD, pGEX5X-1 CIP4/2ΔGBD, or pFLAG-CMV2 CIP4/2ΔGBD, a Quick Change mutagenesis kit was used to change isoleucine residue 454 to serine according to the manufacturer's instructions (Stratagene). All CIP4/2 mammalian expression constructs were confirmed by sequencing and transient expression in COS-1 cells.

Immunoprecipitation and Immunoblotting. Cell lysates were prepared as described (5, 20). The lysates were then incubated with the indicated antibodies for 1 h at 4°C. The immune complexes were precipitated with protein A/G agarose (Santa Cruz Biotechnology) for 1 h at 4°C, washed extensively with lysis buffer, resolved in 4–20% gradient SDS/PAGE, and analyzed by immunoblotting. All immunoblots were developed by enhanced chemiluminesence (Amersham Pharmacia).

***In Vitro* GST Pull-Down Assay.** GST or GST-CIP4/2 fusion proteins were expressed in BL21(DE3)pLysS *Escherichia coli* strain and purified as described (20). Cell lysates were prepared as described above for immunoprecipitation and incubated with either GST alone or GST-CIP4/2 bound to glutathione-Sepharose beads (Amersham Pharmacia) for 2.0 h at 4°C. For GTP binding experiments, cell lysates were incubated with either 1 mM GDP or 100 μM GTPγS for 30 min at 37°C before incubating with GST-fusion proteins (21). The beads were washed five times with lysis buffer, resuspended in 2× sample buffer, subjected to SDS/PAGE, and analyzed by Coomassie blue staining or immunoblotting.

Immunofluorescence Microscopy. For immunofluorescence studies, electroporated cells were processed as described (5, 22). To detect myc-CIP4/2, cells were stained with anti-myc mAb or polyclonal antibody (Santa Cruz Biotechnology) at 2 μg/ml. To detect caveolin, cells were stained with anti-Caveolin polyclonal antibody at 1:500 (Upstate Biotechnology, Lake Placid, NY). To detect HA-TC10, cells were stained with anti-hemagglutinin (HA) mAb (Santa Cruz Biotechnology) at 2 μg/ml. After incubation with primary antibodies, cells were incubated with Alexa^{488} or Alexa^{594} goat anti-mouse or anti-rabbit IgG at 2 μg/ml (Molecular Probes). Coverslips were mounted in Vectashield mounting media (Vector Laboratories). Images were captured by using an Olympus FV 300 confocal microscope, and composite images were generated by using Adobe PHOTOSHOP.

Results

Identification of CIP4/2 as a TC10-Interacting Protein. TC10 is activated after insulin stimulation, and its activation is required for insulin-stimulated glucose uptake and Glut4 translocation (10, 12). To identify TC10 effectors, a yeast two-hybrid cDNA library derived from 3T3L1 adipocytes (16) was screened by using as a bait the constitutively active form of human TC10(Q^{75}L) lacking the C-terminal CAAX domain fused to the DNA binding domain of GAL4. One TC10-interacting clone isolated identified in this screen was a splice variant of human CIP4 (23). The entire insert of the TC10 yeast two-hybrid hit pGADGH CIP4 was sequenced. The TC10-interacting clone contained the coding region of mouse CIP4 encompassing 603 aa including the initiating methionine. Further analysis of the EST database revealed that the mouse CIP4 isolated from the yeast two-hybrid

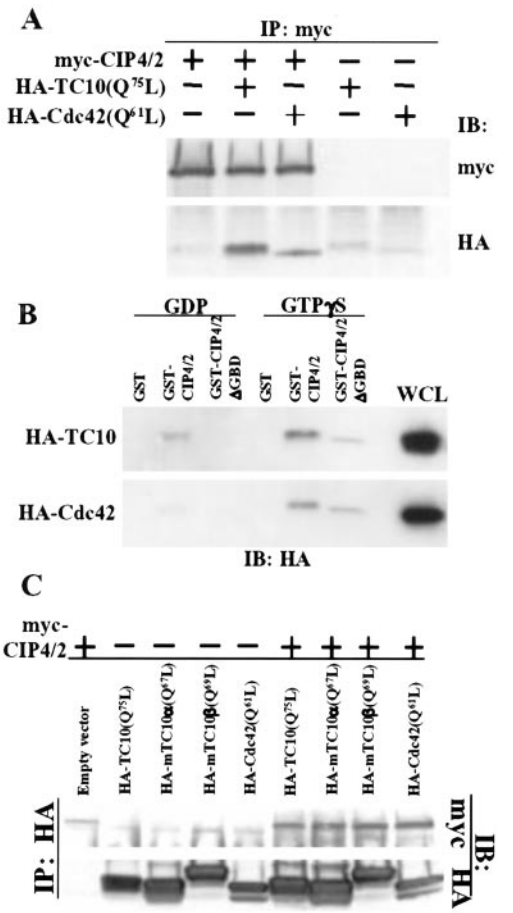

Fig. 1. CIP4/2 interacts with TC10. (*A*) CIP4/2 interacts with TC10 *in vivo*. Cell lysates were prepared from COS-1 cells transfected with myc-CIP4/2, HA-TC10(Q^{75}L), or HA-Cdc42(Q^{61}L) as indicated. Cell lysates were immunoprecipitated with anti-myc antibody. Immunopellets were analyzed by immunoblot analysis using anti-HA or anti-myc antibody. (*B*) CIP4/2 interacts with TC10 in a GTP-dependent manner. Cell lysates were prepared from COS-1 cells transfected with HA-TC10 or HA-Cdc42. Cell lysates were preincubated with either 100 μM GTPγS or 1 mM GDP, and then were incubated with glutathione-Sepharose-bound GST, GST-CIP4/2, or GST-CIP4/2ΔGBD. Precipitates were analyzed by immunoblot analysis with anti-HA antibody. (*C*) CIP4/2 interacts with mTC10α and mTC10β *in vivo*. Cell lysates were prepared from COS-1 cells transfected with myc-CIP4/2, HA-TC10(Q^{75}L), HA-Cdc42(Q^{61}L), mTC10α(Q^{67}L), or mTC10β(Q^{69}L) alone or in combination as indicated. Cell lysates were immunoprecipitated with anti-HA antibody. Immunopellets were analyzed by immunoblot analysis using anti-HA or anti-myc antibody. IB, immunoblotting; IP, immunoprecipitation; WCL, whole-cell lysate.

screen appears to encode a splice variant of human CIP4. Unlike the previously described human CIP4, this clone contained an extra exon encoding 56 aa. The mouse CIP4 splice variant was referred to as CIP4/2, and the mouse ortholog of human CIP4 was referred to as CIP4/1. CIP4/1 and CIP4/2 are essentially identical except for the extra exon encoding 56 aa. Consistent with these data, the alternatively spliced CIP4, CIP4/2, was isolated from mouse heart (GenBank accession no. AY081142). The CIP4/2 sequence that was isolated from the yeast two-hybrid cDNA library derived from mouse 3T3L1 adipocytes has been deposited into GenBank under accession no. AF502565. CIP4/2 is 71% identical to human CIP4 and 74% identical to rat CIP4 with gaps of 10% and 9%, respectively. Consistent with its interaction with constitutively active TC10, human CIP4 was shown to interact with another Rho family member GTPase, Cdc42 (23).

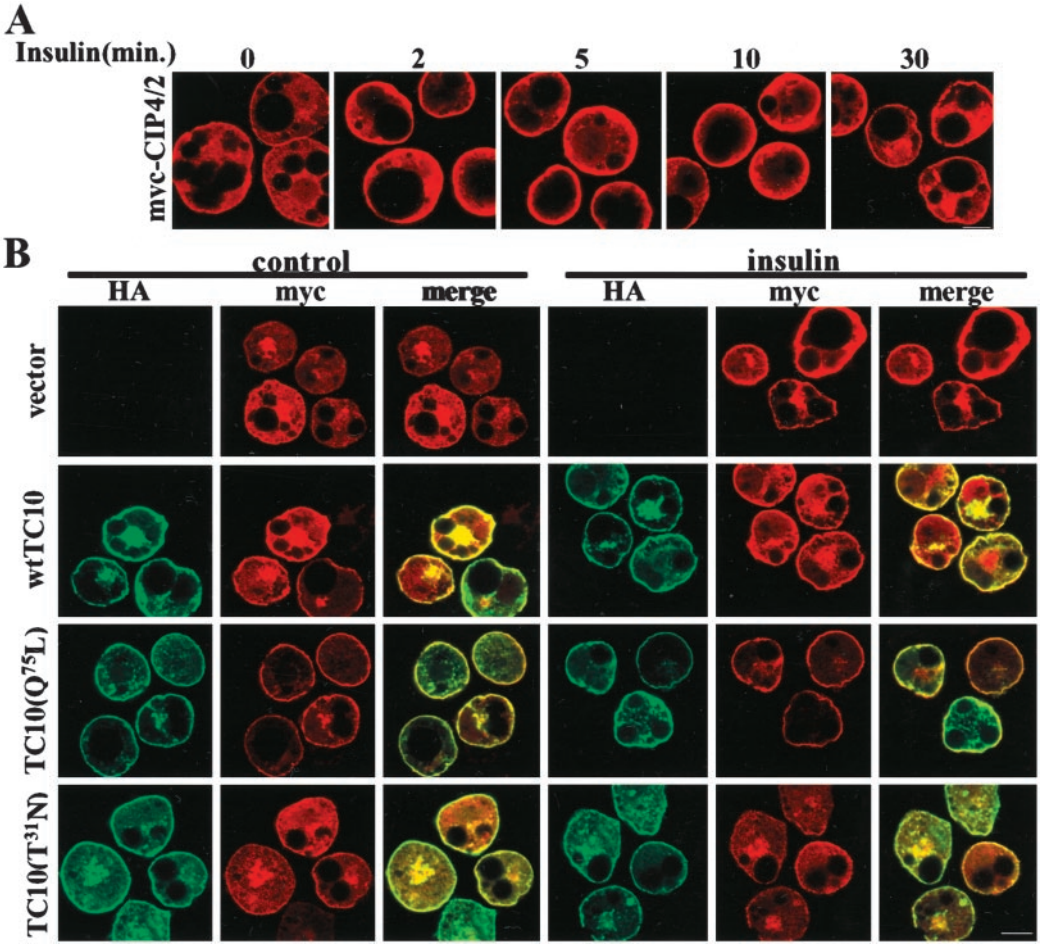

Fig. 2. CIP4/2 immunolocalization. (*A*) CIP4/2 translocates to the plasma membrane in response to insulin. 3T3L1 adipocytes were electroporated with myc-CIP4/2, serum-starved, and treated with or without insulin for the times indicated. Cells were fixed and stained with anti-myc antibody followed by Alexa^{594} goat anti-mouse IgG. (*B*) Overexpression of constitutively active TC10(Q^{75}L) translocates CIP4/2 to the plasma membrane. 3T3L1 adipocytes were coelectroporated with myc-CIP4/2 and vector only, HA-TC10, HA-TC10(Q^{75}L), or HA-TC10(T^{31}N). Serum-starved cells were treated with or without insulin for 5 min, fixed, stained with anti-myc polyclonal antibody to detect myc-CIP4/2 and anti-HA mAb to detect HA-TC10, and followed by Alexa^{594} goat anti-rabbit IgG and Alexa^{488} goat anti-mouse IgG. Fluorescence was visualized by confocal microscopy, and images are representative of four independent determinations. (Bar: 10 μm.)

Previous studies demonstrated the expression of human CIP4 mRNA in insulin-responsive tissues, such as heart and skeletal muscle (23). Mouse CIP4 mRNA was highly expressed in insulin responsive tissues, including high expression in heart and kidney (data not shown). Mouse CIP4 protein was detected in 3T3L1 adipocytes by using anti-CIP4 polyclonal antibodies (ref. 24; generous gift of D. Stewart, National Cancer Institute, Bethesda, MD). The levels of CIP4 protein were similar in preadipocytes and adipocytes, indicating CIP4 protein levels do not change after differentiation (data not shown).

The interaction of CIP4/2 with constitutively active human TC10 (Q^{75}L) was confirmed *in vitro* by using GST-CIP4/2 (data not shown). To confirm the interaction *in vivo*, myc-CIP4/2 and HA-TC10(Q^{75}L) were coexpressed in COS-1 cells. Cell lysates were prepared from transfected cells and immunoprecipitated with anti-myc antibody. As shown previously for human CIP4 (23), mouse myc-CIP4/2 coimmunoprecipitates constitutively active HA-Cdc42(Q^{61}L). Similarly, anti-myc antibody coimmunoprecipitated myc-CIP4/2 with constitutively active HA-TC10(Q^{75}L) (Fig. 1*A*).

To examine whether the interaction between TC10 and CIP4/2 depended on the activation state of TC10, GST-CIP4/2 bound to glutathione-Sepharose was incubated with COS-1 cell lysates expressing TC10 that was preloaded with either GDP or the nonhydrolyzable analog of GTP, GTPγS. The amount of TC10 bound to GST-CIP4/2 was determined by immunoblot analysis (Fig. 1*B*). GST-CIP4/2 bound to the GDP-bound form of TC10 and Cdc42. However, GTPγS-bound TC10 and Cdc42 interacted with much higher affinity, whereas GST did not pull down either Cdc42 or TC10 loaded with GDP or GTPγS (Fig. 1*B*). These data demonstrate that although there is some binding of GDP-bound, inactive TC10 to CIP4, the activation of TC10 increases this interaction.

We recently identified two isoforms of mouse TC10, mTC10α and mTC10β, both of which were activated on stimulation with insulin (10). To examine the interaction of CIP4/2 with mouse TC10 isoforms, myc-CIP4/2 was coexpressed with either constitutively active HA-mTC10α(Q^{67}L) or HA-mTC10β(Q^{69}L) in COS-1 cells. Cell lysates were prepared from transfected cells and immunoprecipitated with anti-HA antibody. Myc-CIP4/2 coimmunoprecipitated with either constitutively active mTC10α(Q^{67}L) or mTC10β(Q^{69}L) (Fig. 1*C*).

CIP4/2 Translocates to the Plasma Membrane in Response to Insulin. The specific interaction of active TC10 with CIP4/2 suggested that insulin might induce a change in the subcellular localization of CIP4/2. To explore this possibility, 3T3L1 adipocytes were transfected with myc-CIP4/2 by electroporation, serum-starved,

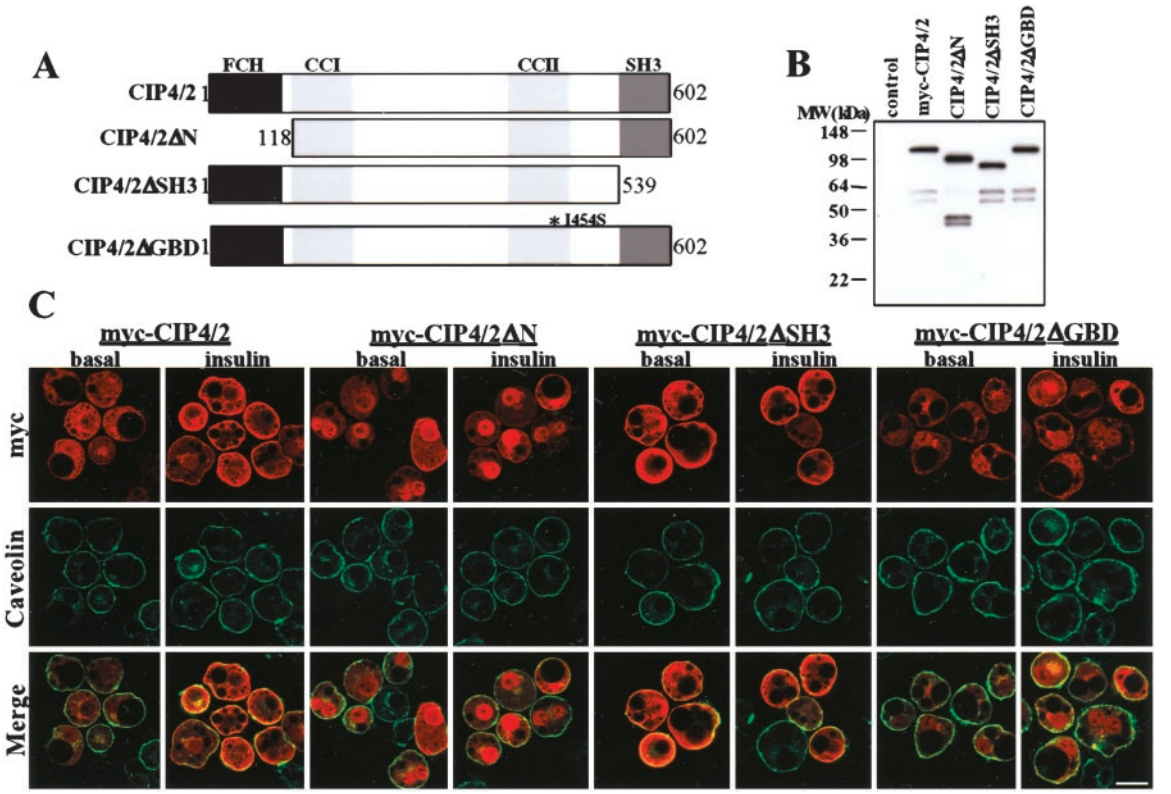

Fig. 3. Immunolocalization of CIP4/2 mutants. (*A*) Schematic of mouse CIP4/2 and its deletion mutants. CIP4/2 contains a FCH, two coiled–coil domains (CC1 and CC2), and SH3. To generate CIP4/2ΔN, the N-terminal 118 aa were deleted. To generate CIP4/2ΔSH3, the C-terminal 63 aa were deleted. To generate CIP4/2ΔGBD, a point mutation was introduced to change isoleucine^{454} to serine indicated as I^{454}S. (*B*) CIP4/2 deletion mutants expressed in 3T3L1 adipocytes. Cell lysates were prepared from 3T3L1 adipocytes electroporated with myc-CIP4/2, myc-CIP4/2ΔN, myc-CIP4/2ΔSH3, and myc-CIP4/2ΔGBD and analyzed by immunoblot analysis using anti-myc antibody. (*C*) 3T3L1 adipocytes were electroporated with myc-CIP4/2, myc-CIP4/2ΔN, myc-CIP4/2ΔSH3, or myc-CIP4/2ΔGBD, serum-starved, and treated with or without insulin for 5 min. Cells were fixed and stained with anti-myc mAb and anti-Caveolin polyclonal antibody followed by Alexa^{594} goat anti-mouse IgG and Alexa^{488} goat anti-rabbit IgG. Fluorescence was visualized by confocal microscopy, and composite images are representative of four independent determinations. (Bar: 10 μm.)

and treated with or without insulin. Cells were fixed and stained with anti-myc antibody to detect myc-CIP4/2 (Fig. 2*A*). There was no specific staining detected with anti-myc antibody in cells electroporated with vector only (data not shown). Under basal conditions, myc-CIP4/2 was diffusely localized throughout the cytoplasm, but was translocated to the cell surface after 1 min of insulin treatment. The protein remained primarily at the plasma membrane through 10 min and began to disassociate by 30 min.

Both TC10α and TC10β localize constitutively at the plasma membrane (10, 25). Because CIP4/2 interacts with TC10 in a GTP-dependent manner, we examined the effects of overexpression of WT, constitutively active, and dominant negative mutants of TC10 on CIP4/2 cellular localization (Fig. 2*B*). On expression in 3T3L1 adipocytes, myc-CIP4/2 was detected primarily in an intracellular compartment (Fig. 2 *A* and *B*). Constitutively active TC10(Q^{75}L) was detected exclusively at the plasma membrane after overexpression. Coexpression of this mutant with CIP4/2 produced the translocation of the latter protein to the plasma membrane. The localization of CIP4/2 in these cells was not further influenced by treatment with insulin (Fig. 2*B*). Similar results were obtained when myc-CIP4/2 was coexpressed with WT TC10 (Fig. 2*B*), consistent with its constitutive localization at the plasma membrane (10, 25). In contrast, a dominant-negative mutant form of TC10(T^{31}N) was detected both in the cytoplasm and the plasma membrane on overexpression, although the basis for this localization pattern is not understood. In contrast to what was observed with the WT or active form of the protein, coexpression of this mutant form of TC10 did not produce a substantial translocation of CIP4/2 to the plasma membrane. Moreover, expression of TC10(T^{31}N) prevented the translocation of CIP4/2 produced by insulin, suggesting that TC10 activation is required for CIP4/2 translocation in these cells.

Overexpression of CIP4/2 Mutants Blocks Insulin-Stimulated Glucose Transport. CIP4/2 contains several protein domains (Fig. 3*A*) (23, 24). The N terminus contains a FER-CIP4 homology (FCH) domain that has been shown to interact with microtubules. The C terminus contains an SH3 domain that may interact with the Wiskott–Aldrich syndrome protein (WASP; ref. 24). In addition, CIP4/2 shows sequence similarity with human FBP17 (formin binding protein 17), similar to human CIP4 (23). There are two predicted coiled–coil regions in CIP4/2. Although human CIP4/2 does not contain a canonical CRIB domain, it has been shown that isoleucine^{398} of human CIP4/2 found within the second coiled–coil domain is essential for Cdc42 interaction (24). Thus, to examine the role of these domains in CIP4/2 localization and function, we generated deletion mutants lacking the N-terminal (CIP4/2ΔN) or C-terminal SH3 domain (CIP4/2ΔSH3), and a point mutant in the second coiled–coil domain that diminishes GTPase binding (CIP4/2ΔGBD) (Fig. 3*A*). To confirm expression of the mutants in mammalian cells, 3T3L1 adipocytes were electroporated with WT myc-CIP4, myc-CIP4/2ΔN, myc-CIP4/2ΔSH3, and myc-CIP4/2ΔGBD. Cell lysates were prepared and analyzed by immunoblot analysis with an anti-myc antibody (Fig. 3*B*). Expression of myc-CIP4/2 and its

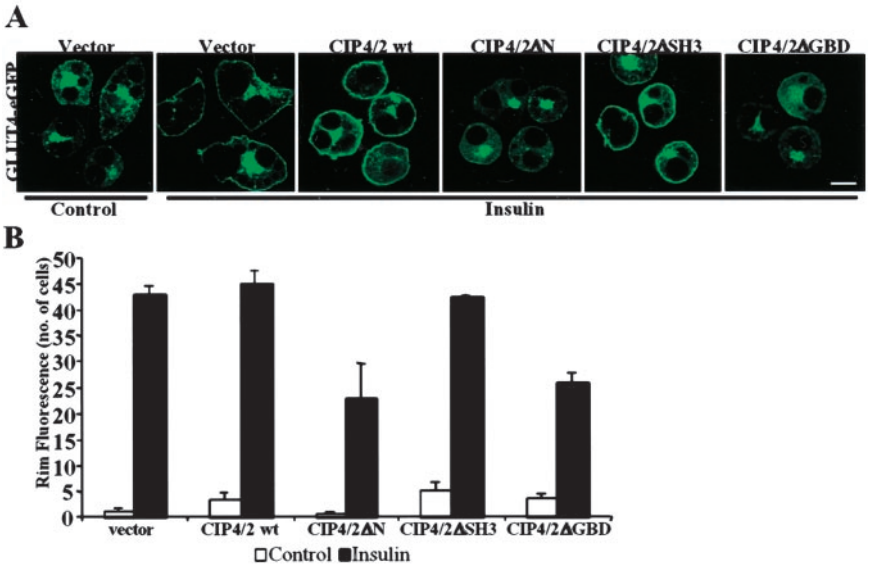

Fig. 4. Effects of overexpression of CIP4/2 and its deletion mutants on insulin-stimulated Glut4 translocation. 3T3L1 adipocytes coelectroporated with GLUT4-eGFP and vector, FLAG-CIP4/2, FLAG-CIP4/2ΔN, or FLAG-CIP4/2ΔGBD were serum-starved, treated with or without insulin for 30 min, fixed and stained with anti-FLAG M2 antibody followed by Alexa^{594} goat anti-mouse IgG to detect cells expressing CIP4/2. Fifty cells expressing FLAG-CIP4/2 or its deletion mutants were scored for visually detectable rim fluorescence before and after treatment with insulin for 30 min. (*A*) Fluorescence was visualized by confocal microscopy, and images are representative of three independent determinations. (Bar: 10 μm.) (*B*) Graphical representation of data from three independent experiments.

deletion mutants were easily detected in 3T3L1 adipocytes (Fig. 3*B*).

Previous studies have shown that human CIP4 interacts with Cdc42 via amino acids 293–481 (23). Further studies showed that mutating isoleucine^{398} to serine abrogated binding to Cdc42 (24). A comparable mouse CIP4/2 mutant was constructed by mutating isoleucine^{454} to serine, generating CIP4/2ΔGBD. Disruption of the putative GTPase binding domain of CIP4/2 was confirmed *in vitro* (Fig. 1*B*).

To determine the role of these domains in defining the subcellular localization of CIP4/2, the deletion mutants were expressed in 3T3L1 adipocytes and detected by immunofluorescence (Fig. 3*C*). Myc-CIP4/2ΔN was detected predominantly in a perinuclear region, suggesting that the N terminus is required for proper targeting of the protein. Interestingly, this mutant did not translocate to the cell surface in response to insulin. Myc-CIP4/2ΔGBD was found in an intracellular compartment in untreated cells, in a distribution similar to that observed with the WT protein. However, this mutant form of CIP4/2 did not translocate to the plasma membrane in response to insulin (Fig. 3*C*). These data are consistent with the decreased affinity of myc-CIP4/2ΔGBD for TC10. Myc-CIP4/2ΔSH3 was constitutively localized to the plasma membrane in the presence or absence of insulin, suggesting that the SH3 domain may interact with another protein that retains CIP4/2 in an intracellular compartment under basal conditions.

To explore the role of CIP4/2 in insulin action, we examined the effect of overexpression of CIP4/2 and its deletion mutants on insulin-stimulated Glut4 translocation. A construct containing a Glut4-eGFP fusion protein was coexpressed with an empty vector, FLAG-CIP4/2, FLAG-CIP4/2ΔN, FLAG-CIP4/2ΔSH3, or FLAG-CIP4/2ΔGBD. To analyze the translocation of Glut4 to the cell surface, cells were scored for eGFP rim fluorescence before and after insulin treatment (Fig. 4). Neither the WT nor mutant forms of CIP4/2 had any effect on the localization of Glut4 in untreated cells. When vector alone was coelectroporated with Glut4-eGFP, 86% of the cells responded to insulin in terms of Glut4-eGFP rim fluorescence. Overexpression of FLAG-CIP4/2 or FLAG-CIP4/2ΔSH3 did not affect Glut4 translocation after insulin treatment (Fig. 4 *A* and *B*). However, overexpression of FLAG-CIP4/2ΔN or FLAG-CIP4/2ΔGBD produced a partial blockade of insulin-stimulated Glut4 translocation, with only 46% or 52% of the cells responding to insulin, respectively. Similarly, FLAG-CIP4/2ΔN or FLAG-CIP4/2ΔGBD inhibited insulin-stimulated translocation of insulin-responsive amino peptidase (IRAP), which has been shown to colocalize in insulin-responsive Glut4-containing vesicles (data not shown) (26, 27). However, neither FLAG-CIP4/2ΔN nor FLAG-CIP4/2ΔGBD had a significant effect on the insulin-stimulated translocation of the cation-independent mannose-6-phosphate receptor (data not shown), confirming the specificity of the inhibition. Interestingly, neither FLAG-CIP4/2ΔN nor FLAG-CIP4/2ΔGBD translocate to the plasma membrane in response to insulin. Together these data indicate that plasma membrane localization of CIP4/2 is essential for insulin-stimulated Glut4 translocation.

Discussion

Two independent, physically separate signaling pathways are required for insulin-stimulated glucose uptake (reviewed in ref. 3). The tyrosine phosphorylation of the insulin receptor substrate proteins induces the activation of PI3-kinase, which in turn stimulates the activity of phosphatidylinositol 3,4,5-trisphosphate-dependent protein kinases such as Akt and atypical forms of PKC. A second pathway involves the tyrosine phosphorylation of the Cbl protooncogene and is independent of the activation of PI3-kinase (22). The Rho family GTPase TC10 is activated by insulin downstream of the phosphorylation of Cbl (10, 12). To examine the role of TC10 in insulin-stimulated glucose transport, we sought to identify effectors of the protein by using a yeast two-hybrid screen with a constitutively active mutant form of TC10($Q^{75}L$) as bait. These efforts resulted in the identification of a splice variant of mouse CIP4, CIP4/2, as a putative TC10 effector. CIP4/2 is a multidomain protein that interacts with TC10 in a GTP-dependent manner.

CIP4/2 exhibits the properties of a key TC10 effector involved in the simulation of glucose transport and Glut4 translocation. Insulin activates TC10 by increasing its GTP-bound state, and

the interaction of TC10 with CIP4/2 is GTP-dependent. Expression of a tagged form of CIP4/2 in 3T3L1 adipocytes revealed that the protein translocates to the plasma membrane in response to insulin. This translocation event can be reproduced by coexpression with constitutively active TC10 and can be blocked by a dominant negative mutant form of TC10, suggesting that, in this context, TC10 activation by insulin is both necessary and sufficient for this step. Finally, overexpression in cells of mutant forms of CIP4/2 can block the stimulation of Glut4 translocation in response to insulin. Taken together, these data suggest that CIP4/2 is an effector for TC10 in the regulation of glucose transport.

The multidomain structure of CIP4 isoforms suggests that this family of proteins may serve an adapter function. CIP4/2 contains an FCH domain, two coiled–coil domains, and an SH3 domain (23). Although the function of the FCH domain is unknown, human CIP4 has been shown to interact with and colocalize with microtubules. Although in preliminary studies we have not been able to detect a direct interaction between CIP4/2 and microtubules (data not shown), it remains possible that other microtubule-associated proteins are required. However, this domain is likely to play an important role in determining the localization of the protein, because the N-terminal portion of CIP4/2 is required for proper localization of the protein in untreated cells, and furthermore CIP4/2ΔN does not translocate to the plasma membrane in response to insulin. Moreover, intact microtubules and a viable actin cytoskeleton are required for membrane localization of CIP4/2 (data not shown), suggesting that intact cytoskeletal architecture is critical for CIP4/2 cellular localization and trafficking.

Coiled–coil domains are known to be involved in protein–protein interactions and can mediate protein dimerization. Interestingly, CIP4/2 does appear to interact with itself (data not shown). The GTPase interacting domain of CIP4/2 appears to reside in its carboxyl-terminal coiled–coil domain, as has been observed for certain other Rho protein effectors (28, 29). Disruption of the CIP4/2 GTPase binding domain inhibited its translocation to the plasma membrane in response to insulin and also blocked insulin–stimulated Glut4 translocation. Taken together, these data suggest that CIP4/2 might function as an adapter to recruit another protein to a subdomain of the plasma membrane via TC10 activation.

One possible region for such an interaction is the SH3 domain of CIP4/2. Deletion of this domain resulted in the constitutive association of the protein with the plasma membrane, suggesting that interaction with another protein might also be important for the intracellular retention of CIP4/2 in untreated cells. In macrophages, human CIP4/2 has been shown to associate with WASP through its SH3 domain, in a manner independent of GTPase activity or GTP binding (24). Although WASP and neural WASP (N-WASP) are highly similar, the expression patterns of the two proteins differ dramatically. WASP is expressed exclusively in hematopoietic cells, whereas N-WASP is ubiquitously expressed (30, 31). Using anti-WASP antibodies, we were not able to detect any WASP expression in 3T3L1 preadipocytes or adipocytes (data not shown). In contrast, we were able to detect N-WASP in both cell types, although we did not observe an interaction between mouse CIP4/2 and N-WASP by *in vitro* or *in vivo* binding analyses (data not shown). Thus, these data indicate that WASP is unlikely to be the binding partner of CIP4/2 that mediates downstream functions of TC10.

Taken together these data suggest that CIP4/2 may act as an adapter protein that recruits additional molecules to the plasma membrane in response to insulin, in the process participating in the translocation of Glut4 to the cell surface. Although the precise role of CIP4/2 in this process is uncertain, one interesting possibility is that CIP4/2 interacts with other proteins at or near the plasma membrane to influence the trafficking of the Glut4 storage vesicle. These interactions may influence the cortical actin cytoskeleton. Indeed, recent studies indicate that remodeling of cortical actin in fat cells has a profound impact on Glut4 trafficking in response to insulin (32), and further that TC10 modulates cortical actin dynamics (33). Alternatively, CIP4/2 may play a role in regulating the docking or fusion of Glut4 at the plasma membrane. These possibilities need further investigation.

We thank Drs. Dom Stewart for anti-human CIP4 polyclonal antibodies, Greg Dressler for pFLAG-CMV2, and Ian Macara for TC10 constructs. We thank Drs. Shian-Huey Chiang and Matthew Wishart for valuable assistance and advice. This work was supported by National Institutes of Health Grant RO1 DK60591.

1. Kelly, K. L., Ruderman, N. B. & Chen, K. S. (1992) *J. Biol. Chem.* **267,** 3423–3428.
2. Kelly, K. L. & Ruderman, N. B. (1993) *J. Biol. Chem.* **268,** 4391–4398.
3. Saltiel, A. R. & Pessin, J. E. (2002) *Trends Cell Biol.* **12,** 65–71.
4. Ribon, V. & Saltiel, A. R. (1997) *Biochem. J.* **324,** 839–845.
5. Liu, J., Kimura, A., Baumann, C. A. & Saltiel, A. R. (2002) *Mol. Cell. Biol.* **22,** 3599–3609.
6. Ribon, V., Printen, J. A., Hoffman, N. G., Kay, B. K. & Saltiel, A. R. (1998) *Mol. Cell. Biol.* **18,** 872–879.
7. Kimura, A., Baumann, C. A., Chiang, S. H. & Saltiel, A. R. (2001) *Proc. Natl. Acad. Sci. USA* **98,** 9098–9103.
8. Baumann, C. A. & Saltiel, A. R. (2001) *BioEssays* **23,** 215–222.
9. Imagawa, M., Tsuchiya, T. & Nishihara, T. (1999) *Biochem. Biophys. Res. Commun.* **254,** 299–305.
10. Chiang, S. H., Hou, J. C., Hwang, J., Pessin, J. E. & Saltiel, A. R. (2002) *J. Biol. Chem.* **277,** 13067–13073.
11. Neudauer, C. L., Joberty, G., Tatsis, N. & Macara, I. G. (1998) *Curr. Biol.* **8,** 1151–1160.
12. Chiang, S. H., Baumann, C. A., Kanzaki, M., Thurmond, D. C., Watson, R. T., Neudauer, C. L., Macara, I. G., Pessin, J. E. & Saltiel, A. R. (2001) *Nature (London)* **410,** 944–948.
13. Brady, M. J., Kartha, P. M., Aysola, A. A. & Saltiel, A. R. (1999) *J. Biol. Chem.* **274,** 27497–27504.
14. Olson, A. L., Knight, J. B. & Pessin, J. E. (1997) *Mol. Cell. Biol.* **17,** 2425–2435.
15. Min, J., Okada, S., Kanzaki, M., Elmendorf, J. S., Coker, K. J., Ceresa, B. P., Syu, L. J., Noda, Y., Saltiel, A. R. & Pessin, J. E. (1999) *Mol. Cell* **3,** 751–760.
16. Printen, J. A., Brady, M. J. & Saltiel, A. R. (1997) *Science* **275,** 1475–1478.
17. Schultz, J., Milpetz, F., Bork, P. & Ponting, C. P. (1998) *Proc. Natl. Acad. Sci. USA* **95,** 5857–5864.
18. Letunic, I., Goodstadt, L., Dickens, N. J., Doerks, T., Schultz, J., Mott, R., Ciccarelli, F., Copley, R. R., Ponting, C. P. & Bork, P. (2002) *Nucleic Acids Res.* **30,** 242–244.
19. Altschul, S. F., Gish, W., Miller, W., Myers, E. W. & Lipman, D. J. (1990) *J. Mol. Biol.* **215,** 403–410.
20. Liu, J., Wu, J., Oliver, C., Shenolikar, S. & Brautigan, D. L. (2000) *Biochem. J.* **346,** 77–82.
21. Benard, V., Bohl, B. P. & Bokoch, G. M. (1999) *J. Biol. Chem.* **274,** 13198–13204.
22. Baumann, C. A., Ribon, V., Kanzaki, M., Thurmond, D. C., Mora, S., Shigematsu, S., Bickel, P. E., Pessin, J. E. & Saltiel, A. R. (2000) *Nature (London)* **407,** 202–207.
23. Aspenstrom, P. (1997) *Curr. Biol.* **7,** 479–487.
24. Tian, L., Nelson, D. L. & Stewart, D. M. (2000) *J. Biol. Chem.* **275,** 7854–7861.
25. Watson, R. T., Shigematsu, S., Chiang, S. H., Mora, S., Kanzaki, M., Macara, I. G., Saltiel, A. R. & Pessin, J. E. (2001) *J. Cell Biol.* **154,** 829–840.
26. Keller, S. R., Scott, H. M., Mastick, C. C., Aebersold, R. & Lienhard, G. E. (1995) *J. Biol. Chem.* **270,** 23612–23618.
27. Kandror, K. V. & Pilch, P. F. (1994) *Proc. Natl. Acad. Sci. USA* **91,** 8017–8021.
28. Maesaki, R., Ihara, K., Shimizu, T., Kuroda, S., Kaibuchi, K. & Hakoshima, T. (1999) *Mol. Cell* **4,** 793–803.
29. Tarricone, C., Xiao, B., Justin, N., Walker, P. A., Rittinger, K., Gamblin, S. J. & Smerdon, S. J. (2001) *Nature (London)* **411,** 215–219.
30. Miki, H., Miura, K. & Takenawa, T. (1996) *EMBO J.* **15,** 5326–5335.
31. Symons, M., Derry, J. M., Karlak, B., Jiang, S., Lemahieu, V., McCormick, F., Francke, U. & Abo, A. (1996) *Cell* **84,** 723–734.
32. Kanzaki, M. & Pessin, J. E. (2001) *J. Biol. Chem.* **276,** 42436–42444.
33. Kanzaki, M., Watson, R. T., Hou, J. C., Stamnes, M., Saltiel, A. R. & Pessin, J. E. (2002) *Mol. Biol. Cell* **13,** 2334–2336.